AGU PUBLICATIONS

Geophysical Research Letters

RESEARCH LETTER
10.1002/2016GL071923

Key Points:
- CMIP5 vertical moisture profiles in the Amazon are too dry compared to observations at low levels, especially during the dry season
- Two modes capture spread in vertical moisture structure, with one mode peaked at low levels and the other in the lower free troposphere
- Comparing these modes to rainfall spread points to inconsistent sensitivity of CMIP5-simulated rainfall to vertical moisture structure

Supporting Information:
- Supporting Information S1

Correspondence to:
B. R. Lintner,
lintner@envsci.rutgers.edu

Citation:
Lintner, B. R., D. K. Adams, K. A. Schiro, A. M. Stansfield, A. A. Amorim Rocha, and J. D. Neelin (2017), Relationships among climatological vertical moisture structure, column water vapor, and precipitation over the central Amazon in observations and CMIP5 models, *Geophys. Res. Lett.*, *44*, doi:10.1002/2016GL071923.

Received 13 NOV 2016
Accepted 1 FEB 2017
Accepted article online 2 FEB 2017

Relationships among climatological vertical moisture structure, column water vapor, and precipitation over the central Amazon in observations and CMIP5 models

Benjamin R. Lintner[1], David K. Adams[2], Kathleen A. Schiro[3], Alyssa M. Stansfield[1], Alciélio A. Amorim Rocha[4], and J. David Neelin[3]

[1]Department of Environmental Sciences, Rutgers, The State University of New Jersey, New Brunswick, New Jersey, USA, [2]Centro de Ciencias de la Atmósfera, Universidad Nacional Autónoma de México, Mexico City, Mexico, USA, [3]Department of Atmospheric and Oceanic Sciences, University of California, Los Angeles, California, USA, [4]Fundação Centro de Análise, Pesquisa e Inovação Tecnológica Faculdade Fucapi, Manaus, Brazil

Abstract Bias and spread in Coupled Model Intercomparison Project Phase 5 simulated vertical specific humidity (q) structure are examined and related to both precipitation and column water vapor (cwv) near Manaus, Brazil, site of the recent Green Ocean Amazon campaign. Simulated seasonal mean q profiles are typically too dry, especially at low levels and during the local dry season, consistent with previously identified surface hydroclimate biases in the Amazon. Multimodel empirical orthogonal function analysis of the models' monthly climatological q profiles indicates two significant modes of ensemble spread in moisture vertical structure, with the leading mode peaked at low levels and the second mode in the lower free troposphere (LFT). While both modes project onto simulated cwv spread, only the first projects on precipitation, suggesting inconsistent sensitivity of simulated rainfall to LFT moisture. Relative to observations, models with high cwv and low-level moisture errors tend to exhibit high precipitation error.

1. Introduction

Encompassing more than half of Earth's tropical rainforest [*Morley*, 2000], the Amazon plays a considerable role in the regulation of the carbon cycle, not to mention the tropical hydrologic cycle and energetics [*Fu et al.*, 1999]. Humans are placing increasing stresses on the Amazon through deforestation, agricultural and industrial development, and resource exploitation. Needless to say, the health of the Amazonian ecosystem and its future outlook are of serious concern, particularly given the potential consequences of anthropogenic climate change. However, current generation model projections remain highly uncertain regarding the future Amazonian climate [*Joetzjer et al.*, 2013].

Coarse-resolution global climate models (GCMs) such as those used in the Coupled Model Intercomparison Project Phase 5 (CMIP5) [*Taylor et al.*, 2012] typically underestimate Amazonian precipitation, especially during the dry season [*Yin et al.*, 2013]. Such models struggle to reproduce the observed precipitation seasonality [*Pascale et al.*, 2014] as well surface energy, water, and biogeochemical fluxes [*de Gonçalves et al.*, 2013]. For instance, while observed surface shortwave radiation, evapotranspiration, and photosynthesis over humid parts of the Amazon are maximized during the dry season [*Restrepo-Coupe et al.*, 2013], in many GCMs, these quantities peak during the wet season [*Pascale et al.*, 2014]. Such deficiencies may fundamentally relate to several aspects of model physics, including land-surface physical or biogeophysical processes [*Gatti et al.*, 2015], convection schemes, entrainment/detrainment, cloud microphysics [*Bechtold et al.*, 2014], and coupling to large-scale circulation [*Yin et al.*, 2013].

While previous studies have diagnosed model errors pertaining to simulation of surface climate over the Amazon, relatively little attention has been devoted to model bias or spread as they relate to vertical structure, especially in moisture. The latter may relate to several model performance issues. Both observational analyses and cloud-resolving model simulations implicate sensitivity of deep convection to free tropospheric humidity [*Grabowski and Moncrieff*, 2004; *Bretherton et al.*, 2004; *Sherwood et al.*, 2004]; however, coarse-resolution GCMs likely underestimate or fail to account for such sensitivity [*Biasutti et al.*, 2006; *Dai*, 2006]. Deep convection is typically triggered too frequently in GCMs, which may reflect insufficient vertical moisture sensitivity [*Kuang and Bretherton*, 2006; *Del Genio*, 2012]. GCM studies provide further evidence that parameters

impacting convective moisture sensitivity, such as entrainment, affect model fidelity in simulating realistic convection behavior, e.g., modes of intraseasonal variability like the Madden Julian Oscillation [*Kim et al*., 2011]. An obvious limitation is the scarcity of observed vertical profiles for validating models. Although progress has been made in recent years to extract vertically profiles from satellite moisture retrievals, these are considered unreliable over land where contamination of the signal from land surface emissivity is problematic [*Deeter*, 2007]. Intense precipitation may also limit microwave retrieval, while clouds affect infrared (IR) retrievals. Radio occultation using Global Positioning System (GPS)/Global Navigation Satellite System (GNSS) [see *Kursinski et al*., 2000] provides vertical moisture structure, but at spatiotemporal resolutions too coarse for evaluating deep precipitating convective conditions.

Within the last 15 years, emergent relationships between column water vapor (cwv) and precipitation in the tropics have been identified from a variety of observations. On subdaily to daily time scales, tropical oceanic precipitation rates derived from satellites have been shown to increase sharply with cwv above a critical value, with properties suggestive of a continuous phase transition [*Bretherton et al*., 2004; *Peters and Neelin*, 2006; *Neelin et al*., 2009]. Focusing on Nauru in the western tropical Pacific, where cwv was estimated from radiosoundings and an in situ radiometer deployed under the Department of Energy's Atmospheric Radiation Measurement program, *Holloway and Neelin* [2009] argued that the cwv-precipitation relationship ultimately stems from the impact of free tropospheric humidity on conditional instability of entraining plumes. To the extent that cwv variability reflects variability of free tropospheric moisture, cwv represents a useful proxy for conditional instability.

Prior work relating high-frequency cwv observations to precipitation has focused on oceanic regions, given the lack of satellite observations over land. However, several recent studies [*Adams et al*., 2013, 2015, 2016; *Schiro et al*., 2016; *Serra et al*., 2016] have analyzed continental cwv available from station-based GPS/GNSS retrievals and intensive field campaigns such as the Green Ocean Amazon (GOAmazon) during 2014–2015 [*Martin et al*., 2016], to derive metrics for evaluating the shallow-to-deep convective transition, deep convective intensity, and spatial scales of moisture covariability. *Schiro et al*. [2016] noted leading order similarity between cwv-precipitation scaling over the central Amazon and tropical western Pacific: as with Nauru [*Holloway and Neelin*, 2009, 2010; *Lintner et al*., 2011], the observed high-frequency variability of cwv in the central Amazon reflects variability in specific humidity (q) over the lower free troposphere (LFT). Of course, how generalizable these land region cwv-precipitation transition statistics are for different regimes, such as sea breeze circulations or regions of complex topography, needs to be assessed, as different settings may exhibit distinct moisture structures and thermodynamic controls on convection.

In this study, we analyze CMIP5 models with respect to vertical moisture structure, cwv, and precipitation in the Amazon, focusing on the vicinity of Manaus, Brazil, for which extensive observations are available, e.g., from GOAmazon. Our study emphasizes behavior at monthly time scales, with the objectives of assessing how well models capture observed vertical moisture structure, identifying patterns of intermodel spread in vertical moisture structure and exploring the implications of deficiencies in model vertical moisture structure for simulated Amazonian climate. Since vertical moisture profiles over land are limited, we also compare simulated and observed cwv. Indeed, the increasing availability of GPS/GNSS-based cwv measurements over tropical land renders cwv a useful quantity for model evaluation.

2. Observations and Models

The radiosonde data analyzed here were obtained from the University of Wyoming Atmospheric Sounding database (http://weather.uwyo.edu/upperair/sounding.html). These data, for site WMO 82332 SBMN Ponta Pelada, Manaus, Brazil, are twice daily (at 0 and 12 UTC, which is +4 h ahead of local time) and span 1999–2013. Prior to analysis, soundings were subjected to a simple quality check procedure. Specifically, soundings with mixing ratios exceeding 3 standard deviations above the mean at a given pressure were flagged for visual inspection. Soundings deemed defective across multiple levels were eliminated, while soundings reporting only a few erroneous levels were maintained but with bad data levels removed. The quality checked soundings were aggregated to monthly means at 25 mb intervals.

CMIP5 model output was downloaded from the Program for Climate Model Diagnosis and Intercomparison (PCMDI) data portal. Given our interest in comparing observations at a single point over land, we selected the CMIP5 model suite forced with prescribed boundary conditions, i.e., the Atmospheric Model Intercomparison

(AMIP)-style simulations. Thirty (30) AMIP-style models were analyzed for 1979–2008; model names and associated acronyms are summarized in the supporting information. Our analysis considers only a single ensemble member for each model.

In addition to pressure level q, we also analyze cwv and precipitation. For our purposes, cwv is defined as the mass weighted integral of q over 925 mb–100 mb, since several models include no values at 1000 mb. Observed precipitation is from monthly $2.5° \times 2.5°$ Climate Prediction Center Merged Analysis of Precipitation (CMAP) [*Xie and Arkin*, 1997] data covering 1979–2008.

3. Results and Discussion

Figure 1 depicts seasonal mean q profiles from radiosonde (solid black lines) and the CMIP5 model ensemble mean (MEM; dashed red lines). For the models, box-and-whiskers illustrate the minimum-maximum and lower-upper quartile ranges and median model value at each pressure. Additionally, insets show seasonal mean values of precipitation and cwv (rectangle for observations; red stars for MEM), with box-and-whiskers again included for the ensemble.

In all seasons, MEM q profiles are too dry compared to observations below ~800 mb, consistent with reported CMIP5 Amazonian dry biases in surface variables like precipitation [*Yin et al*., 2013]. The low-level dry bias is especially pronounced during the dry season (July–September), with models in the lowest quartile spanning a wide range. On the other hand, simulated q values below 800 mb only approach observed values in the upper quartile of models. Interestingly, above 700 mb, during the dry and dry-to-wet transition (October–December) seasons, the MEM is slightly wetter than the observations, and in all seasons, between 25% and 50% of models are wetter than observed. For both seasonal mean cwv and precipitation, MEM values are typically biased low compared to observations. For all seasons except the dry-to-wet transition, cwv in more than 75% of the models is lower than observed. Only 25% of the models produce rainfall exceeding CMAP during the wet season, 25%–50% do in the wet-to-dry transition and dry seasons, and about 50% do in the dry-to-wet transition.

One potential complication with the comparison of observed and simulated specific humidity profiles is differences in the horizontal scales of the CMIP5 models compared to the radiosondes. Over the course of the sonde ascent, some horizontal drift may be introduced, which could benefit the comparison, although this is likely to be small compared to the model grid [*Seidel et al*., 2011]. On the other hand, the spatial decorrelation analysis of cwv observations from a dense network of GPS measurements in the central Amazon by *Adams et al*. [2016] indicates relatively strong moisture spatial covariability across the ~100 km extent of the network, although this covariability may drop sharply during the lead-up to deep convection or in the presence of mesoscale organization.

A further issue is that diurnal variations in q may introduce some systematic differences, since the observed profiles are twice daily, while the simulated profiles represent daily means. The timing of the radiosonde launches at Manaus, at 8 am and 8 pm local time, means that the observed profiles largely miss the daytime boundary layer growth. Vertical mixing of q during the daytime may be expected to decrease moisture in the boundary layer and increase it above. To estimate the impact of such diurnal variations on moisture bias and its vertical structure, we further analyzed the q profiles for the 2 years of GO Amazon data, which were typically four times daily at 1:30 am, 7:30 am, 1:30 pm, and 7:30 pm, with occasional launches at 10:30 am during the wet season. Subtracting the mean of all GO Amazon profiles from the mean of 7:30 am and 7:30 pm soundings for each season indicates that the latter are systematically wetter, by 0.3–0.4 g/kg, below ~975 mb and drier, by up to 0.2–0.3 g/kg over ~975 mb–850 mb, with little systematic difference above. From this, we conclude that the low-level model biases evident in Figure 1 are underestimated, although they would be overestimated in the lowest most model layers, which are not shown.

We next evaluate the spread in AMIP ensemble q profiles by applying a multimodel analysis referred to as principal uncertainty patterns (PUPs) [see *Langenbrunner et al*., 2015; *Lintner et al*., 2016]. For our purposes here, we use empirical orthogonal function (EOF) analysis as the basis for computing PUPs. That is, we compute EOFs on the $M \times N$ matrix comprising $M = 204$ (12 months $\times$ 17 pressures) climatological specific humidity values for $N = 30$ models. Prior to computing the EOFs, the specific humidity field is weighted by the square root of the pressure difference across each model layer to account for differences in mass. The resultant modes (or PUPs) are patterns of intermodel difference, relative to the MEM, ordered from largest

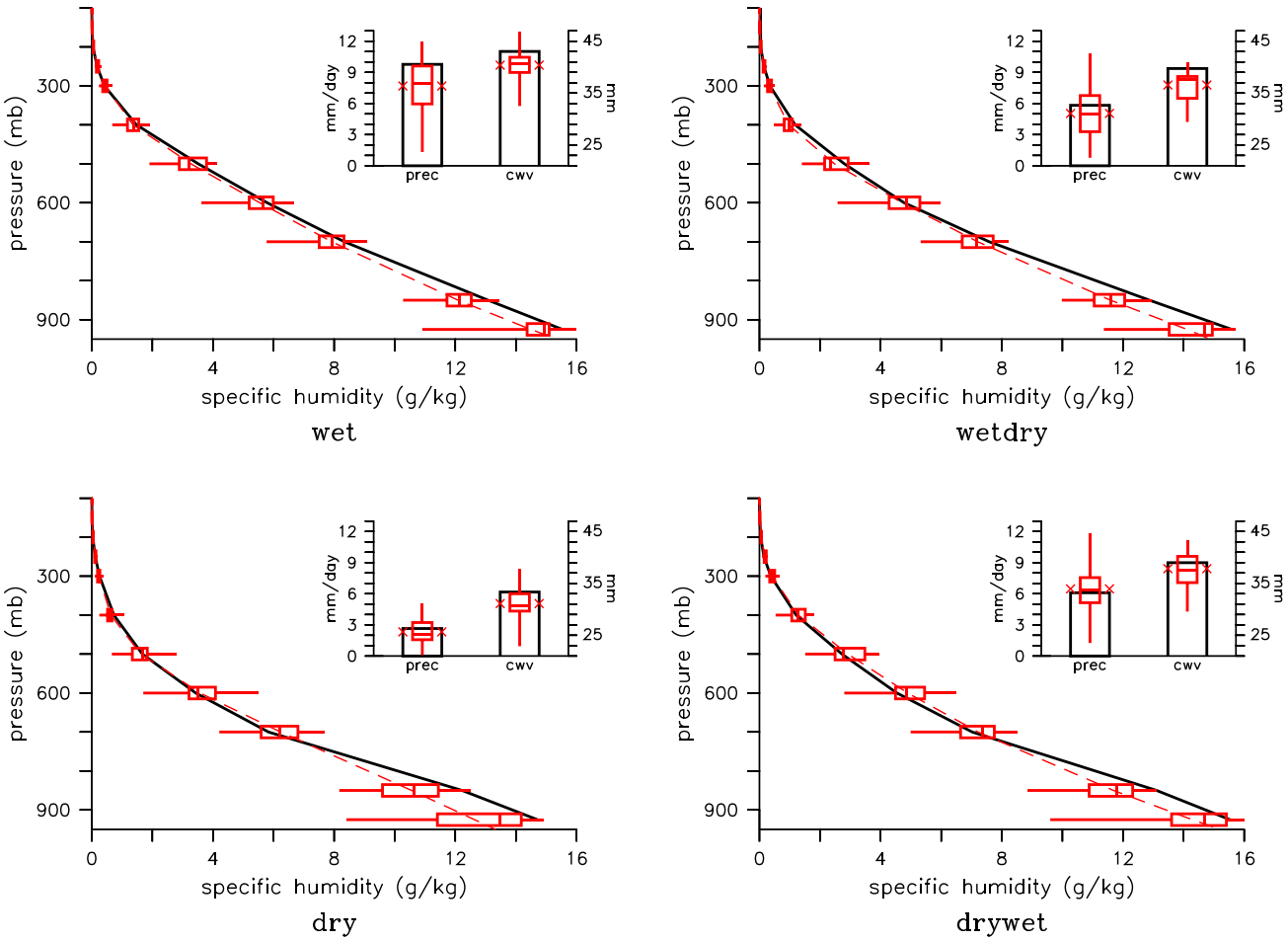

Figure 1. Seasonal mean Manaus q profiles from radiosoundings (thick black line) and the AMIP-style MEM (red dashed line). Box-and-whiskers represent the maximum-minimum and lowest-upper quartile ranges and medians for the ensemble at each pressure. Insets show the seasonal mean observed and simulated precipitation rates, with red stars representing the MEM and box-and-whiskers as before. Seasons are defined following standard definitions at Manaus: wet: January–April; wet-to-dry transition (wetdry): May and June; dry: July–September; and dry-to-wet transition (drywet): October–December.

to smallest in terms of variance explained across the input field. The principal component (PC) associated with each PUP corresponds to weights of individual models onto the EOF, here the 2-D "space" of months and pressure. By construction, the PCs are dimensionless and normalized to unit standard deviation, while the EOFs carry the units of q. We have further computed PUPs on the month × model fields of cwv and precipitation, which we do not show, although we briefly discuss below the correlations of the PCs of these fields with respect to the PCs of q.

The pressure level structure of mode 1 (Figure 2, top left), which accounts for 57% of the total field variance and is significant according to the method of *North et al.* [1982], is effectively of the same sign over the depth of the troposphere across all months, with the exception of values near 700 mb during the dry-to-wet transition. The largest positive values (~2 g/kg) occur at 925 mb during August–October, i.e., the late dry season through early dry-to-wet transition. Not surprisingly, this mode projects strongly onto the leading mode of intermodel spread in cwv ($r = 0.86$; significant at $p > 99\%$ according to a two-tailed Student's t test with 28° of freedom); moreover, it projects strongly onto the leading mode of precipitation spread ($r = 0.78$, $p > 99\%$). The distribution of model weights for the mode 1 (Figure 2, bottom left) displays asymmetry between positive and negative values, as only one model (MRI-CGCM3) exhibits a weight above 1, while five models have weights below −1, i.e., a subset of models is extremely dry compared to the MEM, consistent with Figure 1. Given the presence of outliers, we recomputed PUPs after removing the largest outliers and obtained qualitatively similar results (not shown), indicating robustness for the modes identified.

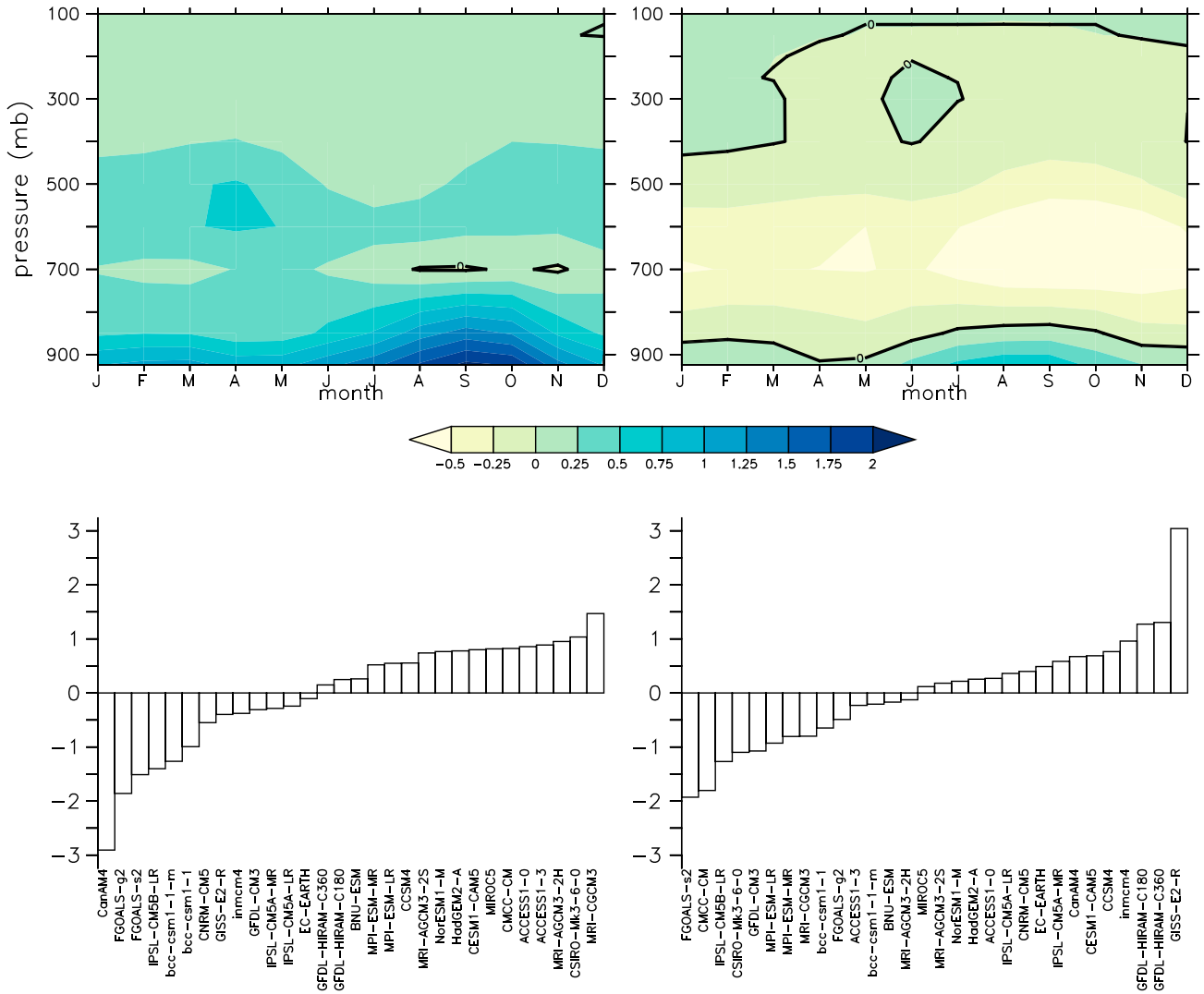

Figure 2. (top row) Multimodel q EOFs (g/kg) and (bottom row) model weights (dimensionless). The first and second modes are on the left and right, respectively.

The second q PUP (Figure 2, top right), which accounts for 21.3% of the total variance and is also deemed significant, is characterized by positive values at 925 mb and mostly negative values above. The largest negative values, occurring between 500 mb–850 mb and exceeding 0.5 g/kg in magnitude, lag the largest positive values below by ~1 month. Interestingly, although the second mode of q projects significantly onto the leading mode of model spread in cwv ($r = 0.51$, $p > 99\%$), it does not project significantly onto the leading mode of precipitation ($r = 0.01$). In other words, the variation across model q structure implied by the second mode significantly impacts the leading mode of intermodel cwv spread, but this does not translate to precipitation, unlike for the leading q PUP. Here we remark that the leading modes of cwv and precipitation spread are themselves correlated at $r = 0.68$, which is slightly less than the direct correlation of leading mode q with precipitation. From this correlation behavior and the vertical moisture structures of the first and second modes, we conclude that particular pressure levels are especially important to determining model spread in precipitation. In particular, the latter is more sensitive to intermodel moisture variation at 925 mb than the layers immediately above.

We now examine how observed and modeled q, cwv, and precipitation fields at Manaus are related by computing the root-mean-square error, RMSE, between observed (obs) and simulated cwv and precipitation for each model (mod) as follows:

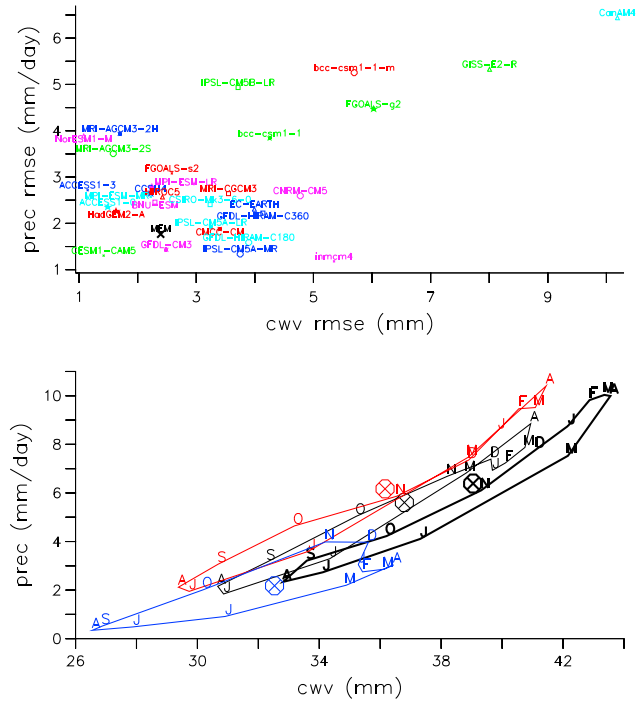

Figure 3. (top) Scatterplot of RMSEs of cwv (*x* axis; in units of mm) and precipitation (*y* axis; in units of mm/d) computed according to equation (1) for each model and the MEM (black cross). (bottom) Monthly cwv-precipitation phase space of the observations (thick black line), MEM (thin black line), highest RMSE subset (blue), and lowest RMSE subset (red). Annual means are denoted by circled crosses.

$$\mathrm{RMSE} = \sqrt{\frac{1}{12}\sum_{i=1}^{12}(\mathrm{obs}_i - \mathrm{mod}_i)^2}, \tag{1}$$

where the sum is performed over all months. This metric accounts for both annual mean biases and biases in seasonal cycle amplitude and phase. A scatterplot of individual model and MEM RMSEs for cwv and precipitation appears in Figure 3 (top). Those models which are high in both cwv and precipitation RMSEs (bcc-csm-1-1, bcc-csm-1-1-m, CanAM4, FGOALS-g2, GISS-E2-R, and IPSL-CM5B-LR) are among the models with the largest dry bias at 925 mb, as seen in Figure 2. GISS-E2-R, the largest positive weight model for the second mode, is the driest model over the LFT. Some models are notable for performing well with respect to one RMSE but not the other. Perhaps unsurprisingly, both cwv and precipitation RMSEs computed with respect to the MEM are lower than for most individual models, although a substantial fraction of the individual models compare favorably to the MEM on one or the other. The MEM is roughly 2 times worse than the either of the best performing models on cwv or precipitation (Nor-ESM1 and inmcm4, respectively). The worst performing model according to these metrics (CanAM4) has RMSEs ~10 times higher than the best performing models.

We further present seasonal phase space plots of cwv and precipitation (Figure 3, bottom) for the observations (thick black curve), MEM (thin black curve), and subsets of models with the highest and lowest RMSEs for precipitation (blue and red, respectively). The highest and lowest RMSE subsets include those models that are either greater than +1 standard deviation above the ensemble mean RMSE (5 models: bcc-csm-1-1-m, CanAM4, FGOALS-g2, GISS-E2-R, and IPSL-CM5B-LR) or less than −1 standard deviation below the ensemble mean RMSE (5 models: CESM1-CAM5, GFDL-CM3, GFDL-HIRAM-C180, inmcm4, and IPSL-CM5A-MR).

Apart from the overall offset in its annual means, the MEM reasonably captures the observed seasonal evolution in cwv-precipitation. The observations indicate separation between wet-to-dry and dry-to-wet transitions, as the former occurs with higher precipitation rates at a given cwv than the latter. A simple interpretation for this separation is that cwv represents only a bulk proxy for instability conditions associated with precipitation occurrence. Thus, aspects of the vertical thermodynamic environment not captured by cwv, such as convective inhibition or the dry intrusions at critical levels, may play a key role. It is also

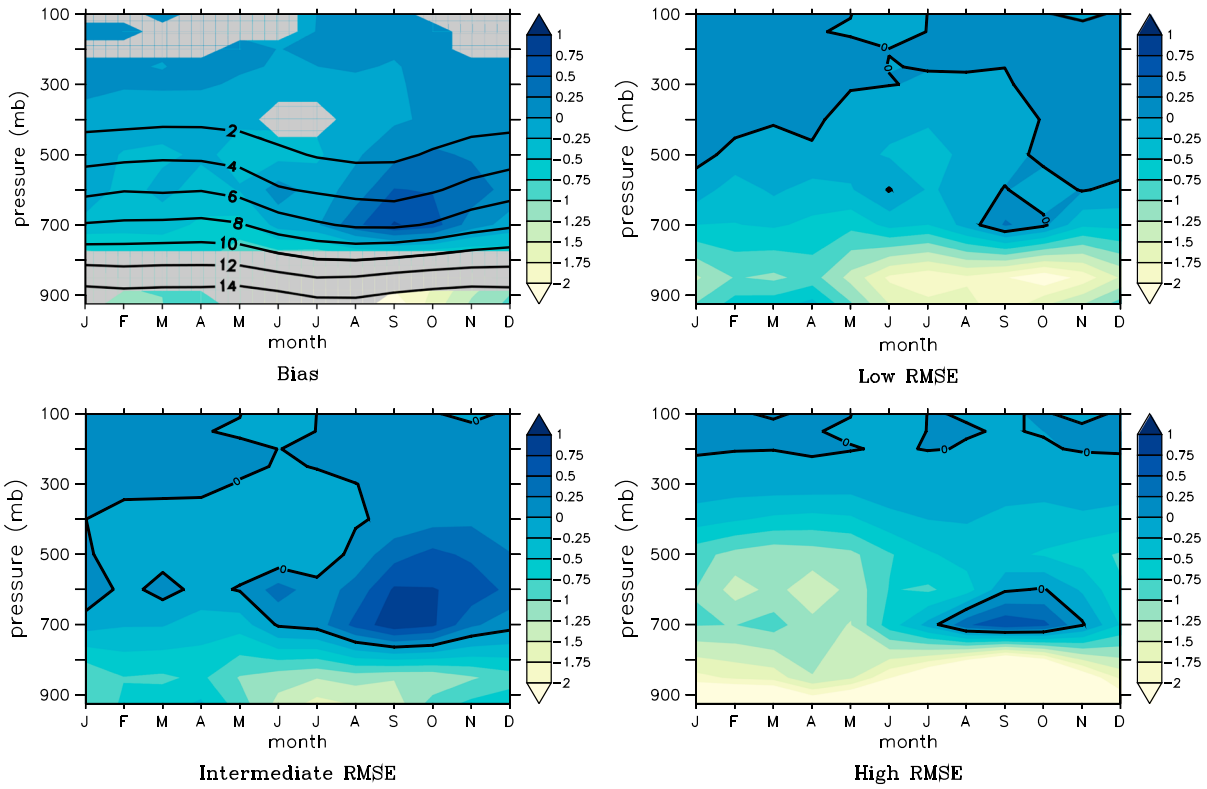

Figure 4. Month pressure cross sections of simulated q biases for (top left) MEM, (top right) lowest RMSE subset, (bottom left) intermediate RMSE subset, and (bottom right) highest RMSE subset. Units are g/kg. For the MEM, line contours show climatological q (in g/kg), and stippling indicates where biases exceed the 1σ level of the MEM.

possible that seasonal differences in cloud processes and microphysics and their relationship to precipitation may modulate the cwv-precipitation relationship. Although it is less distinct, the MEM manifests a similar separation between the transition seasons. The lowest RMSE subset more closely replicates the observed annual mean precipitation, but the November–April values lie along a single branch rather than two branches. The highest RMSE subset is biased low in both cwv and precipitation but, interestingly, manifests a wider separation between the wet-to-dry and dry-to-wet transitions than either the observations or lowest RMSE subset.

Finally, we examine month pressure cross sections of q bias composited with respect to different model subsets (Figure 4). As in Figure 1, the monthly bias of the MEM (top left) tends to be large and negative over 850 mb–925 mb across most of the year, though most prominently in the dry and dry-to-wet transition seasons. The bias exceeds the 1σ level of the MEM in the dry season but not the dry-to-wet transition. Moreover, positive biases occur in the LFT, also consistent with the seasonal view in Figure 1, although they are more prominent in the monthly data, as it is really in August–October, i.e., the *late* dry season/*early* dry-to-wet transition, that these are most prominent. The highest RMSE subset (top right) manifests much larger bias at low levels across all months, with a strong resemblance to PUP mode 1 (we reiterate that models in the highest RMSE subset are among those with the largest negative weights for the first PUP). The vertical structure for the lowest RMSE subset (bottom right) hints at a slightly different structure, with peak negative values at 850 mb instead of 925 mb. The intermediate RMSE subset (bottom left) is notable for having larger LFT positive biases than either the lowest or highest RMSE subsets in the late dry season/early dry-to-wet transition.

4. Summary and Conclusions

We investigated observed and simulated relationships among monthly mean q vertical structure, cwv, and precipitation at Manaus, Brazil, site of the recent GOAmazon field campaign. The seasonal mean vertical q profiles for the 30 CMIP5 models examined are typically dry compared to mean radiosounding profiles, especially below 800 mb and prominently during the dry season. This behavior, mirrored in seasonal dry biases in

cwv and precipitation, is consistent with prior studies of CMIP5-simulated surface hydroclimate biases over the broader Amazon [*Yin et al*., 2013].

By applying multimodel EOF analysis to monthly q profiles, we isolate two modes of ensemble spread in simulated vertical moisture structure at Manaus. The first mode is typically of the same sign throughout the troposphere over all months but strongly peaked at low levels; the second q mode peaks in the layer between 500 mb and 700 mb. Although both modes project significantly onto the leading mode of ensemble spread in cwv (also assessed using EOF analysis), only the leading q mode projects significantly onto the leading mode of spread in precipitation. In light of the vertical structure of the second q mode, the weak correlation to precipitation spread may be indicative of inconsistent sensitivity of simulated rainfall to LFT moisture. In fact, previous work [e.g., *Biasutti et al*., 2006; *Sahany et al*., 2012] indicates that many current convection parameterizations are too weakly dependent on LFT moisture.

Quantifying model agreement with observed precipitation and cwv using a simple RMSE metric indicates a wide range of model skill. Although the MEM outperforms nearly all models with respect to both precipitation and cwv RMSE taken together, many individual models do better than the MEM with respect to either measure individually. It is worth pointing out that previous versions of one of the better performing models for our RMSE measures, CESM1-CAM5, have been shown to perform well in statistics for LFT moisture sensitivity [*Sahany et al*., 2014]. Compositing simulated q profiles with respect to precipitation RMSE performance further indicates that the subset of models with the highest RMSE have the largest biases in low-level moisture, as may be expected. On the other hand, the lowest RMSE models are not those with the smallest biases in the lowest levels; rather, the lowest RMSE subset has smaller biases near 700 mb.

A natural and obvious question to ask is whether the characteristic patterns of spread in vertical moisture structure presented here can be linked to deficiencies or errors in specific processes impacting tropospheric moisture. Although such attribution is beyond the scope of this study, potential sources include entrainment/detrainment, subcloud layer rain re-evaporation, surface energy flux partitioning, and boundary layer thermodynamics and coupling to the LFT, not to mention convection parameterizations themselves. Apart from deficiencies in model physics or parameterizations, some discrepancy may be introduced by differences in the models' native resolution. Finally, given our focus on a single location, we should not discount the possibility that spatial biases in moisture and precipitation account for some aspects of the spread identified here.

Acknowledgments

Data were obtained from the following: CMIP5, PCMDI [http://cmip-pcmdi.llnl.gov/cmip5/data_portal.html]; soundings, the University of Wyoming Department of Atmospheric Science [http://weather.uwyo.edu/upperair/sounding.html]; and CMAP, NOAA/OAR/ESRL PSD, Boulder, Colorado, USA [http://www.esrl.noaa.gov/psd/]. The authors thank Larry D. Oolman of the University of Wyoming for assistance with the soundings, Bryan Raney and Juan Perez Arango for assistance with downloading and formatting CMIP5 output, and Kyle Itterly for useful comments. This work was supported by Department of Energy grants DE-SC0011069 (B.R.L.) and DE-SC0011074 (K.A.S. and J.D.N.) and National Science Foundation grants AGS-1505198 (B.R.L.) and AGS-1540518 (K.A.S. and J.D.N.). A.S.'s participation was partially facilitated through the Rutgers Aresty Undergraduate Research Assistant program.

References

Adams, D. K., S. I. Gutman, K. L. Holub, and D. S. Pereira (2013), GNSS observations of deep convective time scales in the Amazon, *Geophys. Res. Lett.*, *40*, 2818–2823, doi:10.1002/grl.50573.

Adams, D. K., et al. (2015), The Amazon dense GNSS meteorological network: A new approach for examining water vapor and deep convection interactions in the tropics, *Bull. Am. Meteorol. Soc.*, *96*, 2151–2165, doi:10.1175/BAMS-D-13-00171.1.

Adams, D. K., H. Barbosa, and K. De los Rios (2016), A spatiotemporal water vapor/deep convection correlation metric derived from the Amazon Dense GNSS Meteorological Network, *Mon. Weather Rev.*, doi:10.1175/MWR-D-16-0140.1.

Bechtold, P., N. Semane, P. Lopez, J.-P. Chaboureau, A. Beljaars, and N. Bormann (2014), Representing equilibrium and nonequilibrium convection in large-scale models, *J. Atmos. Sci.*, *71*, 734–753, doi:10.1175/JAS-D-13-0163.1.

Biasutti, M., A. H. Sobel, and Y. Kushnir (2006), AGCM precipitation biases in the tropical Atlantic, *J. Clim.*, *19*, 935–958, doi:10.1175/JCLI3673.1.

Bretherton, C. S., M. E. Peters, and L. Back (2004), Relationships between water vapor path and precipitation over tropical oceans, *J. Clim.*, *17*, 1517–1528, doi:10.1175/1520-0442.

Dai, A. (2006), Precipitation characteristics in eighteen coupled climate models, *J. Clim.*, *19*, 4605–4630, doi:10.1175/JCLI3884.1.

de Gonçalves, L., et al. (2013), Overview of the large-scale biosphere–atmosphere experiment in Amazonia Data Model Intercomparison Project (LBA-DMIP), *Agr. Forest Meteor.*, *182/183*, 111–127, doi:10.1016/j.agrformet.2013.04.030.

Deeter, M. N. (2007), A new satellite retrieval method for precipitable water vapor over land and ocean, *Geophys. Res. Lett.*, *34*, L02815, doi:10.1029/2006GL028019.

Del Genio, A. D. (2012), Representing the sensitivity of convective cloud systems to tropospheric humidity in general circulation models, *Surv. Geophys.*, *33*, doi:10.1007/s10712-011-9148-9.

Fu, R., B. Zhu, and R. E. Dickinson (1999), How do atmosphere and land surface influence seasonal changes of convection in the tropical Amazon?, *J. Clim.*, *12*, 1306–1321, doi:10.1175/1520-0442.

Gatti, L. V., et al. (2015), Drought sensitivity of Amazonian carbon balance revealed by atmospheric measurements, *Nature*, *506*, 76–80, doi:10.1038/nature12957.

Grabowski, W. W., and M. W. Moncrieff (2004), Moisture-convection feedback in the tropics, *Q. J. R. Meteorol. Soc.*, *130*, 3081–3104, doi:10.1256/qj.03.135.

Holloway, C. E., and J. D. Neelin (2009), Moisture vertical structure, column water vapor, and tropical deep convection, *J. Atmos. Sci.*, *66*, 1665–1683, doi:10.1175/2008JAS2806.1.

Holloway, C. E., and J. D. Neelin (2010), Temporal relations of column water vapor and tropical precipitation, *J. Atmos. Sci.*, *67*, 1091–1105, doi:10.1175/2009JAS3284.1.

Joetzjer, E., H. Douville, C. Delire, and P. Ciais (2013), Present-day and future Amazonian precipitation in global climate models: CMIP5 versus CMIP3, *Clim. Dyn.*, *41*, 2921–2936, doi:10.1007/s00382-012-1644-1.

Kim, D., A. H. Sobel, E. D. Maloney, D. M. W. Frierson, and I.-S. Kang (2011), A systematic relationship between intraseasonal variability and mean state bias in AGCM simulations, *J. Clim.*, *24*, 5506–5520, doi:10.1175/2011JCLI4177.1.

Kuang, Z., and C. S. Bretherton (2006), A mass-flux scheme view of a high-resolution simulation of a transition from shallow to deep convection, *J. Atmos. Sci.*, *63*, 1895–1909, doi:10.1175/JAS3723.1.

Kursinski, E. R., G. A. Hajj, S. Leroy, and B. Herman (2000), The radio occultation technique, *Terr. Atmos. Ocean Sci.*, *11*, 53–114.

Langenbrunner, B., J. D. Neelin, B. R. Lintner, and B. T. Anderson (2015), Patterns of precipitation change and climatological uncertainty among CMIP5 models, with a focus on the midlatitude Pacific storm track, *J. Clim.*, *28*, 7857–7872, doi:10.1175/JCLI-D-14-00800.1.

Lintner, B. R., C. E. Holloway, and J. D. Neelin (2011), Column water vapor statistics and their relationship to deep convection, vertical and horizontal circulation, and moisture structure at Nauru, *J. Clim.*, *24*, 5454–5466, doi:10.1175/JCLI-D-10-05015.1.

Lintner, B. R., B. Langenbrunner, J. D. Neelin, B. T. Anderson, M. J. Niznik, G. Li, and S.-P. Xie (2016), Characterizing CMIP5 model spread in simulated rainfall in the Pacific Intertropical Convergence and South Pacific Convergence Zones, *J. Geophys. Res. Atmos.*, *121*, 11,590–11,607, doi:10.1002/2016JD025284.

Martin, S. T., et al. (2016), Introduction: Observations and modeling of the Green Ocean Amazon (GoAmazon2014/5), *Atmos. Chem. Phys.*, *16*, 4785–4797, doi:10.5194/acp-16-4785-2016.

Morley, R. J. (2000), *Origin and Evolution of Tropical Rain Forests*, 362 pp., Wiley, London.

Neelin, J. D., O. Peters, and K. Hales (2009), The transition to strong convection, *J. Atmos. Sci.*, *66*, 2367–2384, doi:10.1175/2009JAS2962.1.

North, G. R., T. L. Bell, R. F. Cahalan, and F. J. Moeng (1982), Sampling errors in the estimation of empirical orthogonal functions, *Mon. Weather Rev.*, *110*, 699–706.

Pascale, S., V. Lucarini, X. Feng, A. Porporato, and S. U. Hasson (2014), Analysis of rainfall seasonality from observations and climate models, *Clim. Dyn.*, *44*, 1–21, doi:10.1007/s00382-014-2278-2.

Peters, O., and J. D. Neelin (2006), Critical phenomena in atmospheric precipitation, *Nat. Phys.*, *2*, 393–396, doi:10.1038/nphys314.

Restrepo-Coupe, N., et al. (2013), What drives the seasonality of photosynthesis across the Amazon basin? A cross-site analysis of eddy flux tower measurements from the Brasil flux network, *Agr. Forest Meteor.*, *182/183*, 128–144, doi:10.1016/j.agrformet.2013.04.031.

Sahany, S., J. D. Neelin, K. Hales, and R. B. Neale (2012), Temperature–moisture dependence of the deep convective transition as a constraint on entrainment in climate models, *J. Atmos. Sci.*, *69*, 1340–1358, doi:10.1175/JAS-D-11-0164.1.

Sahany, S., J. D. Neelin, K. Hales, and R. B. Neale (2014), Deep convective transition characteristics in the NCAR CCSM and changes under global warming, *J. Clim.*, *27*, 9214–9232, doi:10.1175/JCLI-D-13-00747.1.

Schiro, K. A., J. D. Neelin, D. K. Adams, and B. R. Lintner (2016), Deep convection and column water vapor over tropical land vs. tropical Ocean: A comparison between the Amazon and the tropical Western Pacific, *J. Atmos. Sci.*, *73*, 4043–4063, doi:10.1175/JAS-D-16-0119.1.

Seidel, D. J., B. Sun, M. Pettey, and A. Reale (2011), Global radiosonde balloon drift statistics, *J. Geophys. Res.*, *116*, D07102, doi:10.1029/2010JD014891.

Serra, Y. L., et al. (2016), The North American monsoon GPS transect experiment 2013, *Bull. Am. Meteorol. Soc.*, doi:10.1175/BAMS-D-14-00250.1.

Sherwood, S. C., P. Minnis, and M. McGill (2004), Deep convective cloud top heights and their thermodynamic control during CRYSTAL-FACE, *J. Geophys. Res.*, *109*, D20119, doi:10.1029/2004JD004811.

Taylor, K. E., R. J. Stouffer, and G. A. Meehl (2012), An overview of CMIP5 and the experiment design, *Bull. Am. Meteorol. Soc.*, *93*, 485–498, doi:10.1175/BAMS-D-11-00094.1.

Xie, P., and P. A. Arkin (1997), Global precipitation: A 17-year monthly analysis based on gauge observations, satellite estimates, and numerical model outputs, *Bull. Am. Meteorol. Soc.*, *78*, 2539–2558.

Yin, L., R. Fu, E. Shevliakova, and R. E. Dickinson (2013), How well can CMIP5 simulate precipitation and its controlling processes over tropical South America?, *Clim. Dyn.*, *41*, 3127–3143, doi:10.1007/s00382-012-1582-y.